http://dx.doi.org/10.35596/1729-7648-2026-24-1-21-29

UDC 621.396.218:614.89.086.5

PROBABILISTIC CHARACTERISTICS OF THE DOWNLINK RADIO CHANNELS SPECTRAL EFFICIENCY IN MACRO-SITES OF 5G MOBILE COMMUNICATIONS

VLADIMIR MORDACHEV

Belarusian State University of Informatics and Radioelectronics (Minsk, Republic of Belarus)

Abstract. Mathematical models for the analysis of probabilistic characteristics of the spectral efficiency of downlink radio channels in macro-sites of mobile (cellular) radio communications have been developed, and estimates of the probability distributions and average values of the potential and real spectral efficiency of downlink radio channels have been made for various variants of the typical IMT-2020 scenarios "Rural-eMBB", "Urban Macro–mMTC" and "Urban Macro–URLLC". Obtained models and estimates take into account the randomness of the user's equipment distribution on the macro-site territory and the possibility of user's equipment location in areas of both free and interference (multi-ray) propagation of radio waves between the base station and user's equipment. These results allow us to conclude that the declarations of new generations of mobile communications in terms of increasing the spectral efficiency of radio channels at the 4G→5G→6G evolution are feasible.

Keywords: mobile (cellular) communications, 5G, eMBB, mMTC, URLLC, spectrum efficiency, base station, user's equipment, downlink radio channel, probability distribution.

Conflict of interests. The author declares that there is no conflict of interests.

For citation. Mordachev V. (2026) Probabilistic Characteristics of the Downlink Radio Channels Spectral Efficiency in Macro-Sites of 5G Mobile Communications. *Doklady BGUIR*. 24 (1), 21–29. http://dx.doi.org/10.35596/1729-7648-2026-24-1-21-29.

ВЕРОЯТНОСТНЫЕ ХАРАКТЕРИСТИКИ СПЕКТРАЛЬНОЙ ЭФФЕКТИВНОСТИ НИСХОДЯЩИХ РАДИОКАНАЛОВ В МАКРОСАЙТАХ СИСТЕМ МОБИЛЬНОЙ РАДИОСВЯЗИ 5G

В. И. МОРДАЧЕВ

Белорусский государственный университет информатики и радиоэлектроники (Минск, Республика Беларусь)

Аннотация. Разработаны математические модели для анализа вероятностных характеристик спектральной эффективности нисходящих радиоканалов в макросайтах систем мобильной (сотовой) радиосвязи, выполнены оценки вероятностных распределений и средних значений потенциальной и реальной спектральной эффективности нисходящих радиоканалов для различных вариантов типовых сценариев IMT-2020 "Rural-eMBB", "Urban Macro–mMTC" и "Urban Macro–URLLC". Полученные модели и оценки учитывают случайность местоположения абонентских терминалов на территории макросайта и возможность присутствия в нем областей как свободного, так и интерференционного (многолучевого) распространения радиоволн между базовой станцией и абонентскими терминалами. Эти результаты позволяют сделать вывод о реализуемости деклараций новых поколений мобильной радиосвязи в части повышения спектральной эффективности радиоканалов в процессе эволюции 4G→5G→6G.

Ключевые слова: мобильная (сотовая) связь, 5G, eMBB, mMTC, URLLC, спектральная эффективность, базовая станция, абонентский терминал, нисходящий радиоканал, распределение вероятности.

Конфликт интересов. Автор заявляет об отсутствии конфликта интересов.

Для цитирования. Мордачев, В. И. Вероятностные характеристики спектральной эффективности нисходящих радиоканалов в макросайтах систем мобильной радиосвязи 5G / В. И. Мордачев // Доклады БГУИР. 2026. Т. 24, № 1. С. 21–29. http://dx.doi.org/10.35596/1729-7648-2026-24-1-21-29.

Introduction

When analyzing scenarios for the implementation of cellular (mobile) communication (MC) systems and services in areas with large site sizes (base station service areas), it is necessary to take into account a large range of possible values of distances between the base station (BS) and user's equipment (UE), randomly distributed over the BS service area. This circumstance is the reason of the large dynamic range of useful signal levels at the inputs of radio receivers of many UEs, determining the values of the *SNIR* parameter – the signal-to-(noise+interference) ratio in the downlink radio channels. The randomness of the UE location relative to the BS is the reason for the randomness of the *SNIR* values and, as a consequence, the randomness of the spectral efficiency W_R [bit/s/Hz] of the "BS-UE" radio channels and its impact on the average wireless area traffic capacity [bit/s/m^2] in the BS service area. The latter determines the relevance of taking into account the randomness of the *SNIR*, W_R values when analyzing the electromagnetic background intensity created by modern and future MC systems, using the methods of [1, 2].

The goal of this paper is to substantiate probabilistic-statistical models and analyze probabilistic-statistical characteristics of the spectral efficiency of "BS-UE" radio channels in macro sites of 5G MC systems when implementing typical IMT-2020 scenarios [3] "Rural-eMBB", "Urban Macro–mMTC" and "Urban Macro–URLLC".

Initial models and expressions

When analyzing probabilistic characteristics of the downlink radio channel spectral efficiency in MC systems with macro-sites of a relatively large area, we use the following well-known models.

1. The macro-site model shown in Fig. 1, in which H_{BS} is the height of the BS antenna phase center above the surface; H_{UE} is the UE height above the surface corresponding to human height; R is a random distance between the BS antenna and an arbitrary UE; R_{BP} is the radius of the BS vicinity, in which the free-space model of radio waves propagation (RWP) between BS and UE can be used ("breakpoint" vicinity); R_m is the distance between the boundary of free-space RWP region and the BS antenna; $R_{\max}$ is the radius of BS service area (macro-site). Typical parameters of this model for macro-sites of IMT-2020 (5G) MC, corresponding to [3], are given in Tab. 1.

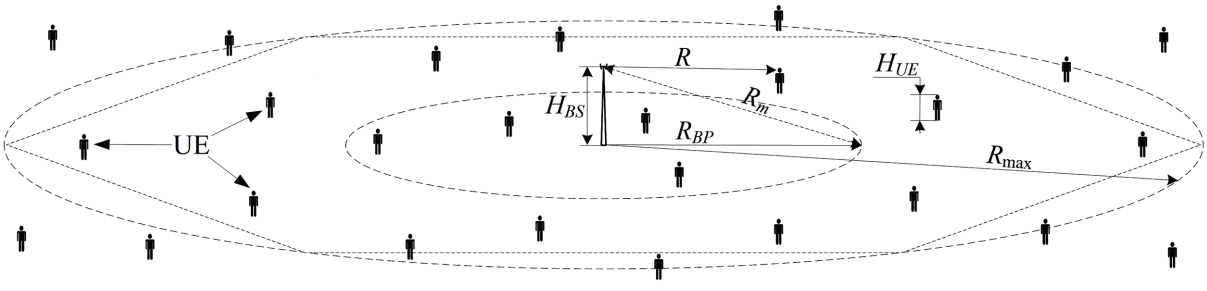

Fig. 1. Macro-site model in the IMT-2020 MC system

Table 1. Macro-site parameters for different options of typical IMT-2020 scenarios

5G Scenario, option No	Configuration	Carrier frequency, GHz/ Wavelength, m	$R_{\max}$ [1)], m	H_{BS}, m	H_{UE}, m	R_{BP}, m
1. Rural-eMBB	A	0.7 / 0.43	1200	35	1.5	490
2. Rural-eMBB	B	4.0 / 0.075	1200	35	1.5	2800
3. Rural-eMBB	C (LMLC)	0.7 / 0.43	4000	35	1.5	490
4. Urban Macro–mMTC	A	0.7 / 0.43	350	25	1.5	350
5. Urban Macro–mMTC	B	0.7 / 0.43	1200	25	1.5	350
6. Urban Macro–URLLC	A	4.0 / 0.075	350	25	1.5	2000
7. Urban Macro–URLLC	B	0.7 / 0.43	1200	25	1.5	350

[1)]Accepted to be equal to 2/3 of the typical value of "Inter-site distance" proposed in [3].

2. Model [4, formula (2)] of the conditions of RWP between BS and UE in the BS service area as the dependence of the power flux density Z [W/m^2] of the electromagnetic field of the BS with the equivalent isotropically radiated power (EIRP) P_e [W] at the point of UE placement, on the distance R from the BS antenna:

$$Z = \begin{cases} \dfrac{P_e}{4\pi R^2} & R \le R_{BP}; \\ \dfrac{R_{BP}^2 P_e}{4\pi R^4} & R > R_{BP}; \end{cases} \qquad R_{BP} = \frac{4H_{UE}H_{BS}}{\lambda}, \tag{1}$$

where λ is the wavelength of BS electromagnetic radiation, m.

As the UE moves away from the BS, the nature of RWP between BS and UE changes. If for $R \le R_{BP}$, the RWP conditions are as in free space, then for $R > R_{BP}$, the conditions of RWP to the UE are determined by the interference of the direct and reflected from the surface rays. The calculated values of R_{BP} radius of the BS "breakpoint vicinity" for various options of macro-sites of typical IMT-2020 scenarios are given in Tab. 1. They allow us to conclude that for options No 2, 4 and 6 $R_{BP} \ge R_{\max}$, which make it possible to use the free-space RWP model (the upper branch of the model (1)) for the entire territory of the macro-site, however, for options No 1, 3, 5 and 7 $R_{BP} << R_{\max}$, and for the large part of the macro-site territory, the interference (multi-ray) model of RWP between BS and UE (the lower branch of the model (1)) must be used. At the same time, for macro-sites, in contrast to 5G micro- and pico-sites, the sizes of which are significantly smaller than the BS "breakpoint vicinity", the difference between the R_{BP} and R_m values is insignificant (less than 0.3 %), which allows us to consider $R_{BP} \approx R_m$.

3. The model of the "BS-UE" radio channel, the potential capacity C_P [bit/s] of which is related to its bandwidth ΔF [Hz] and the potential "signal-to-noise plus interference" $SNIR_P$ in this radio channel by a relationship similar in appearance to the well-known Shannon – Hartley model for an analog communication channel with Gaussian noise:

$$C_P = \Delta F = \log_2\left(1 + SNIR_P\right) = \log_2\left(1 + \frac{P_S}{P_{NI}}\right), \; SNIR_P = \frac{P_S}{P_{NI}}; \; W_P = \frac{C_P}{\Delta F} = \log_2\left(1 + SNIR_P\right), \tag{2}$$

where P_S is the useful signal power in this channel, W; P_{NI} is the total power of noise and intra-system interference in the ΔF band (assuming that the effect of wideband co-channel interference in MC networks on the capacity of their radio channels is similar to the effect of Gaussian noise of the same power), W; W_P is the potential spectral efficiency of data transmission over this radio channel, bit/s/Hz.

The 5G macro-site parameters given in Tab. 1 and model (1) allow us to estimate the expected $SNIR_P$ levels ratio at different UE distances from the BS for the fixed BS EIRP (P_e = const). Estimates of the values of this parameter for R_{BP} and H_{BS} distances, provided that its minimum value $SNIR_{P2\min}$ corresponding to the boundary of the BS service area ($R = R_{\max}$) is 10, are given in Tab. 2.

Table 2. $SNIR_P$ value boundaries for the H_{BS}, R_{BP} and $R_{\max}$ distances between base station and user's equipment

5G Scenario, option No	Configuration	$SNIR_{P2\min}$ ($R = R_{\max}$)	$SNIR_{P2\max}$ ($R = R_{BP}$)	$SNIR_{P1\max}$ [1)] ($R = H_{BS}$)	$SNIR_{P1\max}$, dB ($X = 10$)
1. Rural-eMBB	A	$X = 10$	$Y = X{\cdot}36$	$Y{\cdot}196 = 70\,560$	48.5
2. Rural-eMBB	B	$X = 10$	$R_{\max} \le R_{BP}$	$X{\cdot}1176 = 11\,760$	40.7
3. Rural-eMBB	C (LMLC)	$X = 10$	$Y = X{\cdot}4440$	$Y{\cdot}196 = 8\,700\,000$	69.4
4. Urban Macro–mMTC	A	$X = 10$	$R_{\max} \le R_{BP}$	$X{\cdot}196 = 1960$	32.9
5. Urban Macro–mMTC	B	$X = 10$	$Y = X{\cdot}138$	$Y{\cdot}196 = 271\,000$	54.3
6. Urban Macro–URLLC	A	$X = 10$	$R_{\max} \le R_{BP}$	$X{\cdot}196 = 1960$	32.9
7. Urban Macro–URLLC	B	$X = 10$	$Y = X{\cdot}138$	$Y{\cdot}196 = 271\,000$	54.3

[1)] Estimates of the $SNIR_{P1\max}$ value for BS with sector antennas are optimistic, since their EIRP in the vertical direction is significantly less than in the main lobe; a similar level of useful signal is possible when using in BS adaptive active phased antenna arrays (APAA) "Massive MIMO" in the "Beamforming" mode.

In a real radio channel, due to the imperfection of the encoding/decoding and modulation/demodulation processes, its spectral efficiency is m times lower than the potential one. In order to ensure a data transfer rate equal to C_P in a real radio channel with a spectral efficiency reduced by m times, it is neces-

sary to increase the value of the logarithmic factor in (2) by m times, which is possible due to a corresponding increase in the signal/(noise+interference) ratio to the really necessary $SNIR_R$ level:

$$\left.\begin{aligned} & m\log_2\left(1+SNIR_P\right)=\log_2\left(1+SNIR_R\right)=\log_2\left(\left(1+SNIR_P\right)^m\right);\quad 1+SNIR_R=\left(1+SNIR_P\right)^m; \\ & 1+SNIR_P=\left(1+SNIR_R\right)^{\frac{1}{m}};\quad SNIR_P=\left(1+SNIR_R\right)^{\frac{1}{m}}-1\approx SNIR_R^{1/m};\quad SNIR_R\approx SNIR_P^m. \end{aligned}\right\} \tag{3}$$

Thus, the spectral efficiency W_R of a real radio channel is related to the real value of the $SNIR_R$ by the following relationship:

$$W_R=\frac{W_P}{m}=\frac{\log_2\left(1+SNIR_P\right)}{m}=\frac{\log_2\left(1+SNIR_R\right)^{\frac{1}{m}}}{m}=\frac{\log_2\left(1+SNIR_R\right)}{m^2}\approx\frac{\log_2 SNIR_R}{m^2}. \tag{4}$$

Probabilistic characteristics of the "BS-UE" radio channels spectral efficiency for user's equipment from the base station breakpoint vicinity

With a constant BS EIRP, free space RWP, and a random uniform UE distribution over the BS breakpoint vicinity, the probability distribution density (p.d.d.) $w(P_S)$ of the power of the BS useful signal at the input of the UE radio receivers has the following form [2, 5]:

$$w_1\left(P_S\right)=\frac{P_{\min 1}P_{\max 1}}{\left(P_{\max 1}-P_{\min 1}\right)P_S^2},\quad P_{\min 1}<P_S<P_{\max 1};\quad P_{\min 1}=\frac{\lambda^2 G_{UE}P_e}{16\pi^2 R_{BP}^2},\quad P_{\max 1}=\frac{\lambda^2 G_{UE}P_e}{16\pi^2 R_{BS}^2}, \tag{5}$$

where G_{UE} is the UE antenna gain.

If the power P_S of useful signal at the inputs of UE radio receivers is random, then the potential spectral efficiency W_{P1} of each of the "BS-UE" radio channels with free-space RWP is also random, changing within the following limits:

$$W_{P1}\in\left[W_{P1\min},W_{P1\max}\right],\quad W_{P1\min}=\log_2\left(1+\frac{P_{\min 1}}{P_{NI}}\right),\quad W_{P1\max}=\log_2\left(1+\frac{P_{\max 1}}{P_{NI}}\right); \tag{6}$$

in further analysis, the total noise and interference power in the UE reception band ΔF will be assumed to be constant: $P_{NI}\approx$ const. Due to the monotonic dependence $W_P(P_S)$ in (2), the p.d.d. $w(W_{P1})$ of the potential spectral efficiency of radio channels "BS-UE" of the entire set of UE from BS "breakpoint vicinity" can be determined in the following well-known way:

$$w\left(W_{P1}\right)=w\left(P_S\left(W_{P1}\right)\right)\left|\frac{dP_S\left(W_{P1}\right)}{dW_{P1}}\right|,\quad W_{P1}\in\left[W_{P1\min 1},W_{P1\max}\right], \tag{7}$$

where $P_S(W_P)$ is the inverse function (1) for free-space RWP.

Transformations (7) allows us to obtain the following analytical expression for the p.d.d. of the potential spectral efficiency of the "BS-UE" radio channel for the region $H_{BS}\le R\le R_{BP}$:

$$\left.\begin{aligned} & w\left(W_{P1}\right)=\frac{\left(2^{W_{P1\min}}-1\right)\left(2^{W_{P1\max}}-1\right)\cdot 2^{W_{P1}}\cdot\ln(2)}{\left(2^{W_{P1\max}}-2^{W_{P1\min}}\right)\left(2^{W_{P1}}-1\right)^2},\quad W_{P1}\in\left[W_{P1\min},W_{P1\max}\right]; \\ & W_{P1\min}=\log_2\left(1+\frac{P_{\min 1}}{P_{NI}}\right)=\log_2\left(1+SNIR_{P1\min}\right); \\ & W_{P1\max}=\log_2\left(1+\frac{P_{\max 1}}{P_{NI}}\right)=\log_2\left(1+SNIR_{P1\max}\right); \\ & SNIR_{P1\max}=SNIR_{P1\min}\frac{R_{BP}^2}{H_{BS}^2}=SNIR_{P1\min}\frac{16H_{UE}^2}{\lambda^2}. \end{aligned}\right\} \tag{8}$$

Taking into account the relationship (4) between the potential and real spectral efficiency, using a procedure similar to (7), it is possible to determine the p.d.d. $w(W_{R1})$ and the mathematical expec-

tation $m_1(W_{R1})$ of radio channels "BS-UE" real spectral efficiency for the region $H_{BS} \le R \le R_{BP}$ under the assumption that (4) is constant and does not depend on the UE distance from the BS:

$$\left.\begin{aligned}
&w(W_{R1}) = \frac{\left(2^{mW_{R1\min}} - 1\right)\left(2^{mW_{R1\max}} - 1\right)2^{mW_{R1}} \cdot m \cdot \ln(2)}{\left(2^{mW_{R1\max}} - 2^{mW_{R1\min}}\right)\left(2^{mW_{R1}} - 1\right)^2}, \quad W_{R1} \in \left[W_{R1\min}, W_{R1\max}\right];\\
&W_{R1\min} = \frac{W_{P1\min}}{m} = \frac{\log_2\left(1 + SNIR_{R1\min}\right)}{m^2}; \quad W_{R1\max} = \frac{W_{P1\max}}{m} = \frac{\log_2\left(1 + SNIR_{R1\max}\right)}{m^2};\\
&SNIR_{R1\min} = \left(1 + SNIR_{P1\min}\right)^m - 1 \approx SNIR_{P1\min}^m; \quad SNIR_{R1\max} = \left(1 + SNIR_{P1\max}\right)^m - 1 \approx SNIR_{P1\max}^m;\\
&m_{11}(W_{R1}) = \int_{W_{R1\min}}^{W_{R1\max}} W_{R1} w(W_{R1}) dW_{R1}.
\end{aligned}\right\} \quad (9)$$

Relations (8), (9) characterize the randomness of the "BS-UE" radio channels spectral efficiency in 5G scenarios corresponding to the even options of Tab. 1, for which the RWP conditions in free space correspond to the entire BS service area.

Probabilistic characteristics of the "BS-UE" radio channels spectral efficiency for user's equipment outside the base station breakpoint vicinity

With a constant BS EIRP, multi-ray RWP, and a random uniform UE distribution over the ring area $R_{BP} \le R \le R_{\max}$ outside the BS breakpoint vicinity, the p.d.d. $w_2(P_S)$ and $w_2(SNIR_{P2})$ of the BS useful signal power P_S and the potential ratio $SNIR_{P2}$ at the input of the UE radio receivers, has the following form, determined using the lower branch of model (1) and a procedure similar to (7):

$$w_2(P_S) = \frac{\sqrt{P_{\min 2} P_{\max 2}}}{\left(\sqrt{P_{\max 2}} - \sqrt{P_{\min 2}}\right)2P_S^{3/2}}, \quad P_{\min 2} = \frac{R_{BP}^2 P_e}{4\pi R_{\max}^4} < P_S < P_{\max 2} = P_{\min 1} = \frac{P_e}{4\pi R_{BP}^2}. \quad (10)$$

Then, with the use of a procedure similar to (7), for the considered conditions the type of the p.d.d. $w(W_{P2})$ and $w(W_{R2})$ of potential and real spectral efficiency of the "BS-UE" radio channels for the region $R_{BP} \le R \le R_{\max}$, and also the mathematical expectation $m_1(W_{R2})$ are determined:

$$\left.\begin{aligned}
&w(W_{P2}) = \frac{2^{W_P - 1} \cdot \ln(2) \cdot \sqrt{\left(2^{W_{P2\min}} - 1\right)\left(2^{W_{P2\max}} - 1\right)}}{\left(\sqrt{2^{W_{P2\max}} - 1} - \sqrt{2^{W_{P2\min}} - 1}\right)\left(2^{W_{P2}} - 1\right)^{3/2}}, \quad W_{P2} \in \left[W_{P2\min}, W_{P2\max}\right];\\
&W_{P2\min} = \log_2\left(1 + SNIR_{P2\min}\right); \; W_{P2\max} = \log_2\left(1 + SNIR_{P2\max}\right); \; SNIR_{P2\max} = SNIR_{P2\min}\frac{R_{\max}^4}{R_{BP}^4}.
\end{aligned}\right\} \quad (11)$$

$$\left.\begin{aligned}
&w(W_{R2}) = \frac{2^{mW_{R2}-1} \cdot m \cdot \ln(2) \cdot \sqrt{\left(2^{mW_{R2\min}} - 1\right)\left(2^{mW_{R2\max}} - 1\right)}}{\left(\sqrt{2^{mW_{R2\max}} - 1} - \sqrt{2^{mW_{R\min}} - 1}\right)\left(2^{mW_{R2}} - 1\right)^{3/2}}, \quad W_{R2} \in \left[W_{R2\min}, W_{R2\max}\right];\\
&W_{R2\min} = \frac{\log_2\left(1 + SNIR_{R2\min}\right)}{m^2}; \quad W_{R2\max} = \frac{\log_2\left(1 + SNIR_{R2\max}\right)}{m^2};\\
&SNIR_{R2\min} = \left(1 + SNIR_{P2\min}\right)^m - 1 \approx SNIR_{P2\min}^m; \; SNIR_{R2\max} = \left(1 + SNIR_{P2\max}\right)^m - 1 \approx SNIR_{P2\max}^{\boldsymbol{m}};\\
&SNIR_{P2\min} = \frac{P_{\min 2}}{P_{NI}} = \frac{\lambda^2 G_{UE} R_{BP}^2 P_e}{16\pi^2 P_{NI} R_{\max}^4}, \quad SNIR_{P2\max} = \frac{\lambda^2 G_{UE} P_e}{16\pi^2 P_{NI} R_{BP}^2}; \quad \frac{SNIR_{P2\max}}{SNIR_{P2\min}} = \frac{R_{\max}^4}{R_{BP}^4};\\
&m_{12}(W_{R2}) = \int_{W_{R2\min}}^{W_{R2\max}} W_{R2} w(W_{R2}) dW_{R2}.
\end{aligned}\right\} \quad (12)$$

Relations (11), (12) describe the randomness of the potential and real spectral efficiency of "BS-UE" radio channels for UEs from the interference RWP region under 5G scenarios corresponding to the odd options of Tab. 1. The form of $w(W_{P1})$ and $w(W_{P2})$ for $SNIR_{P1\min} = SNIR_{P2\min} = 10$ and $SNIR_{P1\max}$, $SNIR_{P2\max} \in [10^3, 10^4, 10^5]$ is shown in Fig. 2. The form of $w(W_{R1})$ and $w(W_{R2})$ for $SNIR_{P1\min} = SNIR_{P2\min} = 10$; $SNIR_{P1\max} = SNIR_{P2\max} = 10^3$ and different m are shown in Fig. 3.

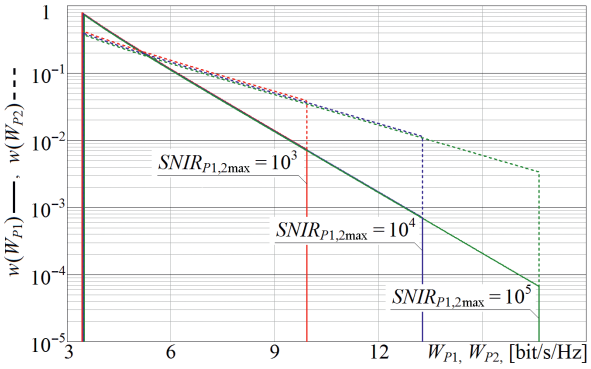

Fig. 2. Curves $w(W_{P1})$ (solid lines) and $w(W_{P2})$ (dashed lines) at $SNIR_{P1\min} = SNIR_{P2\min} = 10$ and $SNIR_{P1\max}$, $SNIR_{P2\max} \in [10^3, 10^4, 10^5]$

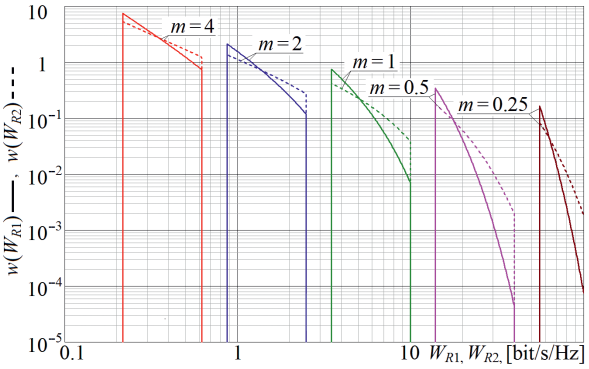

Fig. 3. Curves $w(W_{R1})$ (solid lines) and $w(W_{R2})$ (dashed lines) at $SNIR_{P1\min} = SNIR_{P2\min} = 10$; $SNIR_{P1\max} = SNIR_{P2\max} = 10^3$ and $m \in [0.25, 4]$

Probabilistic characteristics of the "BS-AT" radio channels spectral efficiency for the entire base station service area at $R_{BP} < R_{\max}$

If in the BS service area $R_{BP} < R_{\max}$, and it contains areas with different RWP conditions, then at a uniform random distribution of UEs over its territory with a constant average density ρ_{UE} [UE/m^2], the p.d.d. $w(W_P)$ of the potential and $w(W_R)$ of the real spectral efficiency of "BS-UE" radio channels can be obtained using (8), (9), (11) and (12):

$$w(W_P) = w(W_{P1})\frac{R_{BP}^2}{R_{\max}^2} + w(W_{P2})\frac{R_{\max}^2 - R_{BP}^2}{R_{\max}^2}; \quad W_{P1} \in [W_{P1\min}, W_{P1\max}], \; W_{P2} \in [W_{P2\min}, W_{P2\max}], \quad (13)$$

where

$$W_{P1\min} = \log_2(1 + SNIR_{P1\min}), \quad W_{P1\max} = \log_2(1 + SNIR_{P1\max}); \quad SNIR_{P1\max} = SNIR_{P1\min}\frac{R_{BP}^2}{H_{BS}^2};$$

$$W_{P2\min} = \log_2(1 + SNIR_{P2\min}); \; W_{P2\max} = \log_2(1 + SNIR_{P2\max}); \; SNIR_{P2\max} = SNIR_{P2\min}\frac{R_{\max}^4}{R_{BP}^4};$$

$$SNIR_{P2\min} = SNIR_{P\min}, \; SNIR_{P2\max} = SNIR_{P\min}\frac{R_{\max}^4}{R_{BP}^4} = SNIR_{P1\min}; \; SNIR_{P1\max} = SNIR_{P\min}\frac{R_{\max}^4}{R_{BP}^2 H_{BS}^2};$$

$$w(W_R) = w(W_{R1})\frac{R_{BP}^2}{R_{\max}^2} + w(W_{R2})\frac{R_{\max}^2 - R_{BP}^2}{R_{\max}^2}; \quad W_{R1} \in [W_{R1\min}, W_{R1\max}], \; W_{R2} \in [W_{R2\min}, W_{R2\max}], \quad (14)$$

where

$$SNIR_{R2\min} = (1 + SNIR_{P2\min})^m - 1; \; SNIR_{R2\max} = (1 + SNIR_{P2\max})^m = SNIR_{R1\min};$$

$$SNIR_{R1\min} = (1 + SNIR_{P1\min})^m - 1; \quad SNIR_{R1\max} = (1 + SNIR_{P1\max})^m - 1;$$

$$W_{R2\min} = \frac{\log_2(1 + SNIR_{R2\min})}{m^2}; \quad W_{R2\max} = W_{R1\min} = \frac{\log_2(1 + SNIR_{R2\max})}{m^2} = \frac{\log_2(1 + SNIR_{R1\min})}{m^2};$$

$$W_{R1\max} = \frac{W_{P1\max}}{m} = \frac{\log_2(1 + SNIR_{R1\max})}{m^2}; \; m_1(W_R) = \int_{W_{R2\min}}^{W_{R1\max}} W_R w(W_R) dW_R; \; P(W_{R0}) = \int_{W_{R2\min}}^{W_{R0}} w(W_R) dW_R.$$

Using the data from Tab. 2, we'll perform an analysis for options No 1, 3, 5, 7 of typical IMT-2020 scenarios, which are characterized by the presence of an interference RWP region in the BS service area. Fig. 4–6 contain the curves of the probability distribution function (p.d.f.) $P(W_{R0})$ presented in (14) for these options for different $m \in [0.25, 4]$ under the assumption that for the UEs at the boundary of the BS service area, the actual $SNIR_{R2\min} = 10$ (10 dB), and its actual values for UEs at the outer and inner boundaries of the free-space RWP region correspond to the calculated values $SNIR_{P2\max}$ and $SNIR_{P1\max}$ in Tab. 2. Fig. 7 shows the dependencies of the mathematical expectation $m_1(W_R)$ given in (14), for all options from Tab. 1, 2.

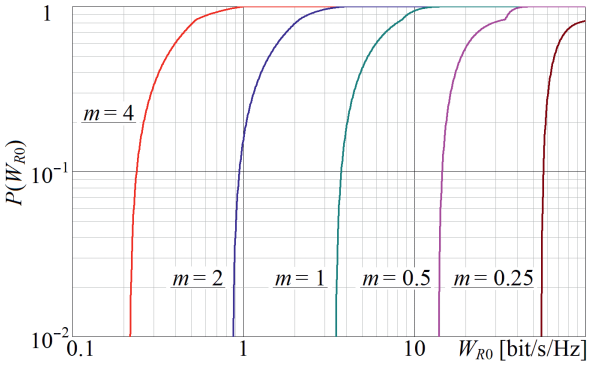

Fig. 4. Curves of p.d.f. $P(W_{R0})$ at different m for macro-sites of option No 1 of typical 5G scenarios

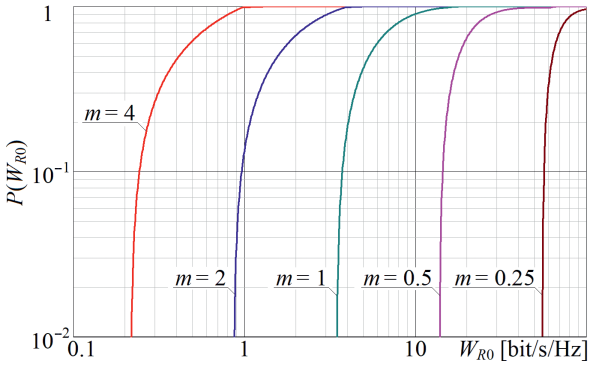

Fig. 5. Curves of p.d.f. $P(W_{R0})$ at different m for macro-sites of option No 3 of typical 5G scenarios

Analysis of the calculated dependencies in Fig. 2–7 indicates the following.

1. The p.d.d. of potential and real spectral efficiency for sets of UE distributed over the freespace RWP region and over the interference RWP region are identical in shape; the difference in the steepness of the decline of their peak is due to the difference in the degree of P_S in (5) and (10).

2. Curves of the p.d.f. $P(W_{R0})$ for different options of typical 5G scenarios at the same values of m, differ relatively little; the kinks in these curves for $m \le 1$ are due to the limited adequacy of model (1) at distances $R \approx R_{BP}$, where a sudden significant change in the RWP conditions is declared upon transition from the region $R < R_{BP}$ to the region $R > R_{BP}$.

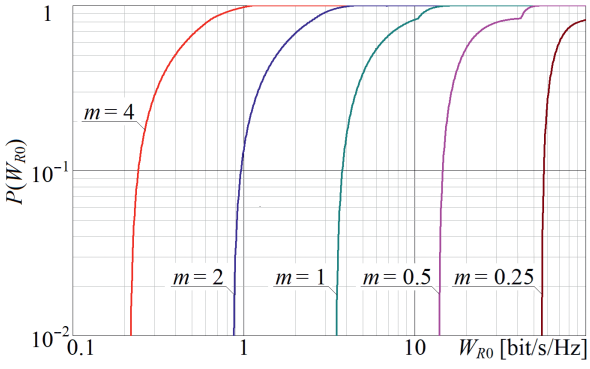

Fig. 6. Curves of p.d.f. $P(W_{R0})$ at different m for macro-sites of options No 5, 7 of typical 5G scenarios

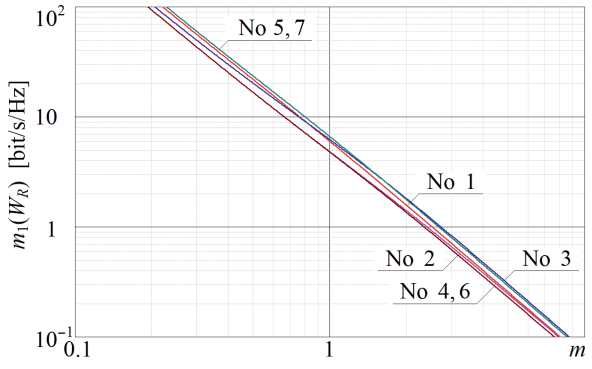

Fig. 7. Dependencies of mathematical expectation $m_1(W_R)$ on m for macro-sites of options No 1–7 of typical IMT-2020 scenarios from Tab. 1, 2

3. Under the adopted conditions of radio reception of BS signal at the boundary of the service area ($SNIR_{R2\min} = 10$), the mathematical expectation of real spectral efficiency at m = const depends relatively little on the scenario option (scattering of values of the "average spectral efficiency per macro-site" $m_1(W_R)$ for different options does not exceed 1.25–1.50), but, as expected, strongly depends on m, which determines the difference in the potential and real spectral efficiency of "BS-UE" radio channels. In Fig. 7, the lower curve for all m corresponds to options 4 and 6, which are characterized by the lowest value of $SNIR_{R1\max}$ for UEs located near the BS. For $m \ge 2$, the highest spectral efficiency corresponds to option 3, in which values of signal/(noise + interference) ratio for UEs in the area of free-space RWP

are maximum. For $m < 2$, the highest spectral efficiency corresponds to options 5 and 7, characterized by a large difference in values of $R_{\max}$ and R_{BP}, which, due to dependence (1), determines large levels of the useful signal for UEs in free-space RWP region.

4. Models (8), (9), (11)–(14) presented above allow to obtain only a general introduction of the spectral efficiency probabilistic-statistical characteristics of downlink radio channels of the MC macro-sites, since they are obtained under the assumption of the BS EIRP constancy for all UEs in the BS service area and the BS receiving path operation in the linear mode for any dynamic range of input signals. In real MC radio networks, the BS EIRP cannot be the same for all UEs, at least due to the use of sector antennas with a complex shape of their radiation patterns in the horizontal and vertical planes within the corresponding sector of the BS service area (this difference can be leveled only by the use of the "Massive MIMO" APAA in the "Beamforming" mode [6] or self-focusing APAA [7] in MC BS). In a number of modes of MC radio networks operation, the BS radiation power adjustment in "BS-UE" radio channels is used, which requires the introduction of appropriate changes in models (5), (10) and can significantly affect the form and characteristics of the above probabilistic models. In addition, at very high levels of the useful signal at the UE input, the spectral efficiency of data transmission over the "BS-UE" radio channel can be limited due to nonlinear effects of various nature in the UE receiving path.

Conclusion

1. The models of probabilistic-statistical characteristics of the spectral efficiency of "BS-UE" radio channels in macro sites of the MC systems obtained in this paper, illustrated in relation to the implementation options of the typical 5G scenarios "Rural-eMBB", "Urban Macro–mMTC" and "Urban Macro–URLLC", allow us to draw a conclusion about the feasibility of declarations [8, 9] in terms of a multiple increase in spectral efficiency of radio channels at evolution 4G→5G→6G.

2. If in MC radio channels without using MIMO technology $m \approx 2$–10 [10], then in 5G systems MIMO technology provides a gain in spectral efficiency of 2–8 times [11], for 6G systems the growth of radio channels spectral efficiency is declared to be 5–10 times compared to 5G systems [9], and, in general, due to MIMO technology, the spectral efficiency of MC radio channels can be ensured at least at the level of 10-20 bit/s/Hz [12]. Such a level of spectral efficiency on average for 5G macro-sites corresponds to $m \approx 0.5$ (under the conditions adopted above in the analysis), which is quite achievable at the modern technological level.

References

1. Mordachev V. I. (2019) Estimation of Intensity of Electromagnetic Background, Created by Wireless Systems of Public Information Services, on the Base of Forecast of Traffic Terrestrial Density. *Doklady BGUIR*. (2), 39–49. https://doklady.bsuir.by/jour/article/view/1066 (in Russian).
2. Mordachev V. (2024) Radiofrequency Electromagnetic Pollution of the Habitat Created by Mobile Communications. *Biology Bulletin*. 51 (11), 3481–3495. DOI: 10.1134/S1062359024701863 (Pleiades Publishing, Inc., USA).
3. *Guidelines for Evaluation of Radio Interface Technologies for IMT-2020* (2017). Report ITU-R M.2412-0.
4. *Propagation Data and Prediction Methods for the Planning of Short-Range Outdoor Radiocommunication Systems and Radio Local Area Networks in the Frequency Range 300 MHz to 100 GHz*. Rec. ITU-R. 1411–11.
5. Mordachev V. (2009) System Ecology of Cellular Communications. *Belarus State University Publishers*. https://emc.bsuir.by/m/12_116413_0_176480.pdf (in Russian).
6. Asplund H., Astely D., Butovitsch P., Chapman T., Frenne M., Chasemzadeh F., et al. (2020) Advanced Antenna Systems for 5G Network Deployments. Bridging the Gap Between Theory and Practice. *Academic Press.*
7. Loyka S. L., Mordachev V. I. (1998) On Applications of Self-Phased Array Antennas to Mobile *Communications. 1998 IEEE Radio and Wireless Conf. (RAWCON'98), Colorado Springs. Colorado, Aug. 9–12.* 233–236.
8. *IMT Vision – Framework and Overall Objectives of the Future Development of IMT for 2020 and Beyond*. Rec. ITU-R M.2083-0.
9. Zhang Z., Xiao Y., Ma Z., Xiao M., Ding Z., Lei X., et al. (2019) 6G Wireless Networks: Vision, Requirements, Architecture, and Key Technologies. *IEEE VT Magazine*. 14 (3), 28–41.

10. Tikhvinskiy V., Terentiev S., Visochin V. (2014) *LTE/LTE Advanced Mobile Networks: 4G Technologies, Applications Architecture*. Moscow, Media Publ. (in Russian).
11. *LTE-Advanced (3GPP Rel.12). Technology Introduction*. White Paper (2015) 1ma252_wp_lte_rel12_2e.pdf. Available: https://www.rohde-schwarz.com/us/applications/lte-advanced-3gpp-rel-12-technology-introduction-white-paper-white-paper_230854-108294.html (Accessed 2 July 2025).
12. Oestges C., Clerckx B. (2010) MIMO Wireless Communications – From Real-World Propagation to Space-Time Code Design. *Claude Academic Press*.

Received: 2 July 2025 Accepted: 23 December 2025

Information about the author

Mordachev V., Cand. Sci. (Tech.), Associate Professor,
Head of the R&D Laboratory “Electromagnetic Compatibility of Radioelectronic Equipment”,
Belarusian State University of Informatics and Radioelectronics

Address for correspondence

220013, Republic of Belarus,
Minsk, P. Brovki St., 6
Belarusian State University
of Informatics and Radioelectronics
Tel.: +375 17 293-84-38
E-mail: mordachev@bsuir.by
Mordachev Vladimir